Transition Met Chem (2014) 39:939–949
DOI 10.1007/s11243-014-9879-9

A kinetic study of aqua ligand substitution in dinuclear Pt(II) complexes containing four non-coplanar pyridine ligands

Grace Kinunda · Deogratius Jaganyi

Received: 4 July 2014 / Accepted: 2 September 2014 / Published online: 30 September 2014
© Springer International Publishing Switzerland 2014

Abstract Substitution reactions of the aqua ligands from azine-bridged dinuclear platinum(II) complexes of the type [{*cis*-Pt(py)$_2$(OH$_2$)}$_2$(μ-pzn)](ClO$_4$)$_4$ [pzn = pyrazine (**Pt-PZN**), 2,3-dimethylpyrazine (**Pt-2,3PZN**), 2,5-dimethylpyrazine (**Pt-2,5PZN**) or 2,6-dimethylpyrazine (**Pt-2,6PZN**)] by thiourea nucleophiles were investigated under *pseudo* first-order conditions as a function of concentration and temperature using the stopped-flow technique. The experimental results are discussed in reference to structures obtained by DFT calculations. The results are in good agreement with the p*K*a values of the complexes as well as DFT calculations. Compared to [{*cis/trans*-Pt(NH$_3$)$_2$(OH$_2$)}$_2$(μ-pzn)](ClO$_4$)$_4$, the complexes in this series react faster by a factor of 10 or 23 respectively due to the presence of pyridine rings, which forces the geometry to allow π-back bonding to take place such that the electrons from the metal centres are accepted to the empty π^*-orbitals of the pyridine subunits. The reactivity of the nucleophile is sterically dependent, with *N*,*N*,*N*′,*N*′-tetramethylthiourea reacting three times slower than thiourea. In all complexes and for both substitution steps, the mode of activation remains associative in nature.

Introduction

In order to understand how dinuclear Pt(II) complexes interact with biological molecules, it has become increasingly important to understand the mechanism of their ligand substitution reactions using model molecules which mimic bionucleophiles such as thios, certain groups of enzymes, peptides and proteins. Kinetic investigations of Pt(II) complexes may contribute to a better understanding of the rates of important biochemical transformations as well as the underlying mechanisms. In particular, by monitoring the substitution reactions with sulphur donors, more information can be gained on the possible modes of interaction of Pt(II) complexes with in vivo targets and their subsequent application in the study of their anti-tumour properties.

Kinetic studies of the ligand substitution of dinuclear Pt(II) complexes with flexible and rigid linkers have been reported [1–12]. The reactivity of the metal centres has been shown to depend on the length and nature of the bridging ligand [1–12]. For example, when a straight aliphatic chain is used in dinuclear complexes with monodentate ammine [8] and bis(2-pyridylmethyl)amine [1, 9–12] carrier ligands around the Pt centres, the reactivity increases with the increase in chain length until it reaches the point where it is independent of the chain length. This observation was ascribed to the decrease in charge addition of the Pt atoms caused by a combination of increased electrostatic interactions with a concomitant increase in the σ-donor capacity towards each Pt atom [1, 2]. A similar trend in reactivity was observed by van Eldik et al. [1, 9–12] when anionic and biologically relevant nucleophiles were used to study the ligand substitution reactions in alkanediamine-bridged Pt(II) complexes with a bis(2-pyridylmethyl)amine chelate framework around each Pt atom. The trend in reactivity is the same in all known cases as that reported in the study by Jaganyi et al. [8] for dinuclear complexes with monodentate amine ligands around the Pt(II) centres. In addition, a decrease in reactivity with an

Electronic supplementary material The online version of this article (doi:10.1007/s11243-014-9879-9) contains supplementary material, which is available to authorized users.

G. Kinunda · D. Jaganyi (✉)
School of Chemistry and Physics, University of KwaZulu-Natal, Scottsville 3209, South Africa
e-mail: jaganyi@ukzn.ac.za

increase in alkanediamine chain was observed for dinuclear complexes with the linker in the *cis*-position relative to the leaving group [13]. This trend is attributed to the strong σ-donor ability of the $-(CH_2)_n-$ moiety that is in the *cis*-position with respect to the leaving group. This causes accumulation of the electron density at the metal centre, making it less electrophilic [13]. On the other hand, when rigid and semi-rigid ligands are used to link Pt(II) centres, the reactivity of the complex depends on the ability of the linker to decrease the electron density at the metal centre through π-back bonding [5, 7, 14].

The substitution results obtained for dinuclear Pt(II) complexes show that their reactivities may be manipulated by the geometry of the complex, especially with respect to the relationship of the leaving group to the diamine bridge, and the nature of the diamine bridge itself as well as the other ligands in the Pt coordination sphere. It has been reported that the DNA binding properties of Pt(II) complexes differ dramatically when the ligand coordinated to the Pt centre is varied from NH_3 to pyridine [15]. The current study is an expansion of earlier work from our group on azine-bridged dinuclear Pt(II) complexes with NH_3 ligands *cis* or *trans* to each other [7, 14] and is intended to resolve the thermodynamic and kinetic properties of the complexes as a function of pyridine ligands bonded to the Pt centre. We are particularly interested to know whether the pyridine rings will enter into electronic communication with the Pt(II) orbitals through π-backbonding and how will this affect the reactivity of the complexes, taking into account the steric effects of the methyl groups on the pyrazine linker. For this reason, we set out to synthesize and study the kinetics of ligand substitution of novel cationic dinuclear Pt(II) complexes bearing two pyridine rings at each Pt centre (Fig. 1). The choice of the pyridine ligand and azine as a linker was due to the interesting cytotoxic activities of their mononuclear and dinuclear Pt(II) complexes [15–18].

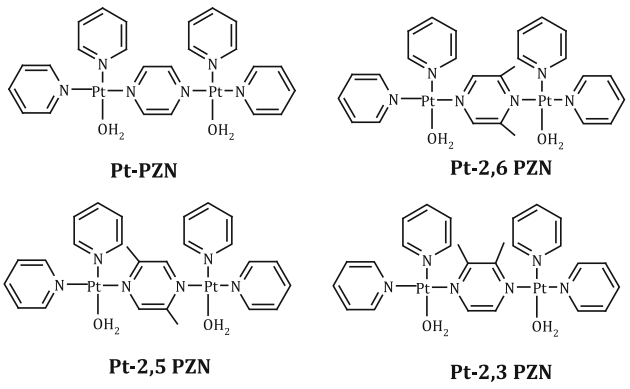


Fig. 1 Structures of the complexes investigated in this study (charges omitted for clarity)

Experimental

Chemicals and reagents

Pyrazine (99 %), 2,3-dimethylpyrazine (99 %), 2,5-dimethylpyrazine (99 %), 2,6-dimethylpyrazine (99 %), $NaClO_4{\cdot}H_2O$ (98 %), $HClO_4$ (70 %), $AgClO_4$ (99.98 %) and pyridine (99 %) were obtained from Aldrich and used without further purification. Potassium tetrachloroplatinate [$K_2(PtCl_4)$] (99.99 %) was purchased from Strem. Thiourea, TU (99 %), 1,3-dimethyl-2-thiourea, DMTU (99 %), 1,1,3,3-tetramethyl-2-thiourea, TMTU (98 %) used in the kinetic measurements were obtained from Aldrich. Ultrapure water (PureLab Systems) was used in all experiments. All other reagents used were of analytical grade quality.

Synthesis of *trans*-[$PtCl_2Py_2$]

The mononuclear starting compound of general formula [*trans*-$PtCl_2(Py)_2$] was prepared according to a literature procedure [19]. To a solution of K_2PtCl_4 (1.62 g, 3.89 mmol) in water (100 mL) was added pyridine (1.25 mL, 15.58 mmol), and the mixture was heated at reflux temperature until the yellow precipitate which formed redissolved to give a clear solution. HCl (2.0 M, 100 mL) was added to the hot solution, and the mixture heated at reflux until the solution turned yellow. On reducing the volume of the solution to ca 10 mL, a light yellow solid precipitated. This was filtered off and washed with water and acetone. The crude product was recrystallized from $CHCl_3$/ether.

***trans*-[$PtCl_2Py_2$]** Light yellow powder, yield 1.44 g (89 %). ^{1}H NMR ($CDCl_3$, 400 MHz,): $\delta = 8.92$ (d, 4H), 7.79 (t, 2H), 7.32 (t, 4H). ^{13}C NMR ($CDCl_3$, 400 MHz,): 153.7, 138.3 and 125.2. Anal. Calcd. for $C_{10}H_{10}N_2PtCl_2$: C 28.3, H 2.4, N 6.6. Found C 28.3, H 2.4, N 6.5. TOF MS ES$^+$: *m*/*z*, $[M + Na]^+ = 446.97$.

Synthesis of [*trans*-{$PtCl(Py)_2(DMF)$}]ClO_4

The title compound was prepared following the literature method [20–22]. To a solution of a known amount of *trans*-[$PtCl_2(Py)_2$] in DMF (10 mL) was added one equivalent of $AgClO_4$. The solution was stirred in the dark overnight at room temperature. After cooling to 5 °C, the precipitated AgCl was filtered off and the yellow filtrate retained.

Synthesis of dinuclear Pt(II) complexes

The synthesis of the new tetrapyridyl coordinated dinuclear complexes was adopted from a previously published method [22] starting with [*trans*-{$PtCl(Py)_2(DMF)$}]ClO_4 and pyrazine derivatives as the bridging ligand, with some

minor modifications. To a filtrate of [*trans*-{$PtCl(Py)_2(DMF)$}]ClO_4 was added dropwise a solution of the pyrazine derivative (half equivalent that of the metal complex) in DMF (2 mL). The mixture was stirred overnight at 30–40 °C in the dark. The solution was then cooled and concentrated on a rotary evaporator at reduced pressure to a volume of approximately 2 mL. The off-yellow compounds that precipitated out after the addition of methanol (20 mL) was filtered off and repeatedly recrystallized from minimal H_2O/ethanol. All complexes were prepared as perchlorate salts and characterized by ^1H NMR and elemental analysis. Characterization data were in excellent agreement with the proposed structures.

Pt-PZN Light yellow powder, yield 76.60 mg (35 %). ^1H NMR (DMSO-d_6, 400 MHz,): $\delta = 8.95$ (d, 2H), 8.79 (d, 8H), 8.02 (t, 4H), 7.73 (d, 2H), 7.53 (dd, 8H). *Anal. Calcd*. for $C_{24}H_{24}N_6O_8Pt_2Cl_4$: C 27.3, H 2.6, N 7.9. *Found* C 27.6, H 2.5, N 7.6.

Pt-2,3PZN Light yellow powder, yield 74.40 mg (33 %). ^1H NMR (DMSO-d_6, 400 MHz,): $\delta = 8.97$ (d, 8H), 8.94 (d, 2H), 8.22 (t, 4H), 7.76 (dd, 8H), 2.35 (s, 6H). *Anal. Calcd*. for $C_{26}H_{28}N_6O_8Pt_2Cl_4$: C 28.8, H 2.6, N 7.7. *Found* C 28.2, H 2.8, N 7.5.

Pt-2,5 PZN Light yellow powder, yield 67.64 mg (30 %). ^1H NMR (DMSO-d_6, 400 MHz,): $\delta = 8.95$ (d, 8H), 8.39 (s, 2H), 8.19 (t, 4H), 7.74 (dd, 8H), 2.43 (s, 6H). *Anal. Calcd*. for $C_{26}H_{28}N_6O_8Pt_2Cl_4$: C 28.8 H 2.6, N 7.7. *Found* C 28.7, H 2.5, N 7.6.

Pt-2,6 PZN Light yellow powder, yield 67.64 mg (30 %). ^1H NMR (DMSO-d_6, 400 MHz,): $\delta = 8.74$ (s, 2H), 8.96 (d, 8H), 7.81 (t, 4H), 7.32 (dd, 8H), 2.61 (s, 6H). *Anal. Calcd*. for $C_{26}H_{28}N_6O_8Pt_2Cl_4$: C 28.8, H 2.6, N 7.7. *Found* C 29.1, H 2.6, N 7.7.

Preparation of solutions for kinetic analysis

The desired solutions of the diaqua complexes were prepared by reacting a known amount of chloro Pt(II) complex with $AgClO_4$ in a molar ratio of 1:1.98 molar respectively in 0.1 M $HClO_4$. The mixture was vigorously stirred in the dark at 50 °C for 24 h. After cooling in ice, the precipitated AgCl was filtered off with a 0.45-μm nylon membrane filter using a Millipore filtration apparatus. The resulting aqueous solution was diluted with 0.1 M $HClO_4$ to a final complex concentration of 3.4×10^{-4}, 2.15×10^{-4}, 4.37×10^{-4} and 5.78×10^{-4} M for **Pt-PZN**, **Pt-2,3PZN**, **Pt-2,5PZN** and **Pt-2,6PZN**, respectively.

Instrumentation and measurements

NMR spectra were recorded on a Bruker Avance III 500 spectrometer at 500 MHz using either a 5-mm BBOZ probe or a 5-mm TBIZ probe. All proton chemical shifts are quoted relative to the relevant solvent signals at 30 °C. Elemental compositions of the complexes were determined with a Carlo Erba Elemental Analyzer 1106. The pH values of aqueous solutions of the complexes were measured using a Jenway 4330 Conductivity/pH meter equipped with a Micro 4.5 diameter glass electrode. The electrode was calibrated at 25 °C using standard buffer solutions of pH 4.0, 7.0 and 10.0 (Merck). The pH electrode was filled with 3.0 M NaCl rather than KCl to prevent the precipitation of $KClO_4$. An Applied Photophysics SX 20 stopped-flow spectrophotometer thermostated to within ±0.1 °C was used for the kinetic measurements. pK_a and kinetic traces were graphically analysed using the software package, Origin 7.5® [23].

Computational methods

The geometry optimizations of the complexes **Pt-PZN**, **Pt-2,3PZN**, **Pt-2,5PZN** and **Pt-2,6PZN** were carried out in water at the DFT level B3LYP [24] with LanL2DZ basis set [25] using the Gaussian 09 program suite and the CPCM formalism [26–28]. B3LYP relates to the hybrid functional Becke's three-parameter formulation, which has been proven to be superior to traditional functionals. LANL2DZ is double-zeta basis set containing effective core potential (ECP) representations of electrons near the nuclei for transition metal complexes [29]. The complexes were optimized in their diaqua form as cations of total charge +4, and the singlet states were used due to low electronic spin of Pt(II) complexes.

pK_a titrations of the diaqua complexes

Spectrophotometric pH titrations of solutions of the aqua complexes were performed using NaOH as the base in the pH range of 1–10 at 25 °C. In order to avoid absorbance corrections due to dilution, a large volume (150 mL) of the metal complex solution was used during the titration. Adjustments in pH were made by stepwise additions of crushed solid NaOH pellets in the pH range 1–3, while micropipette dropwise additions of NaOH solutions of different concentrations (1.0, 0.5, 0.1 and 0.01 M) or 1 M HClO4 (for reversibility of the pH) were added to the solution in the pH range of 4–10 until the desired pH was attained prior to withdrawal of a 1.0 mL aliquot from the solution for pH measurement and 2 mL aliquots for spectrophotometric monitoring the absorbance. The 1 mL aliquot after each pH measurement was discarded to avoid in situ contamination of the complex solution by chloride ions leaching from the pH electrode.

Kinetic measurements

The kinetics of the substitution of coordinated aqua ligands of the complexes **Pt-PZN**, **Pt-2,3PZN**, **Pt-2,5PZN** and **Pt-2,6PZN** were monitored under *pseudo* first-order conditions with at least a 20-fold excess of the nucleophile concentration over the dinuclear complex at pH 2 in order to force the reactions to go to completion. The reactions were initiated by mixing equal volumes of a solution of the Pt(II) complex with a solution of the nucleophile directly in the stopped-flow instrument at suitable wavelengths, predetermined from UV–Vis spectrophotometry (**Table SI 1**). Observed rate constants, k_{obs1} and k_{obs2} were calculated by a double exponential fit to the kinetic traces. The reported k_{obs1} and k_{obs2} are mean values of at least five independent kinetic runs on the stopped-flow spectrophotometer. The second-order rate constants, k_1 and k_2, were obtained by a fit of a straight line to the plot of k_{obs1} and k_{obs2} versus concentration of nucleophile, [Nu] using a standard least-squares minimizing procedure by Origin 7.5® software package [23]. The temperature dependencies of the rate constants in the range of 15–35 °C at a 5 °C intervals allowed for calculation of the enthalpies and entropies of activation, $\Delta H^{\neq}$ and $\Delta S^{\neq}$, with the nucleophile concentration held constant at 60 times the concentration of the metal complex. The respective values were obtained by a linear fit of the natural logarithm of the second-order rate constant, $\ln\left(k_{1/2}/T\right)$ versus $1/T$ using Eyring's equation [30].

Results

Computational analysis

In this study, one of the most important structural parameters is the presence of two pyridine moieties *trans* to each other and *cis* to the leaving group at each Pt(II) centre. Calculations were performed in order to gain an in-depth understanding of the structural as well as the electronic differences that exist in these complexes compared to those reported in previous studies [7, 14]. Geometry-optimized structures and the HOMO/LUMO maps are shown in Table 1, while the selected metric data are presented in Table 2.

It is important to mention that the complexes were synthesized and are drawn as *trans*, but at the end of the calculation, the pyridine rings had twisted to the equatorial plane, adopting the *cis* geometry in relation to the second pyridine ring. The calculations also show that the square planarity around the Pt centres is maintained and the pyrazine ligand plus the twisted pyridine rings all lie on the same plane with the Pt(II) centres creating an environment for electronic communication through π-backbonding.

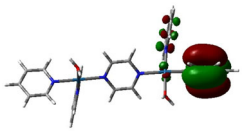
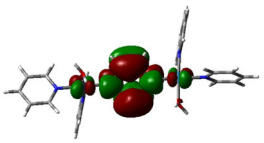
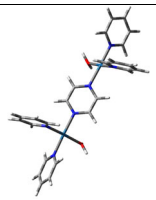
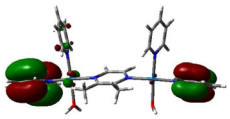
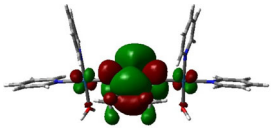
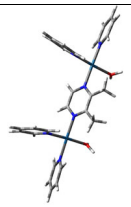
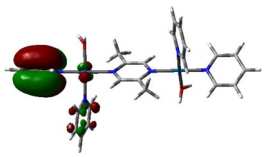
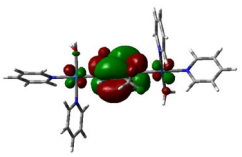
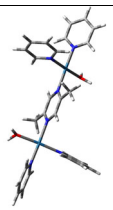
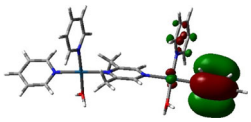
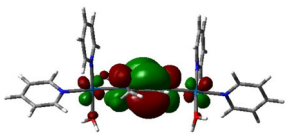
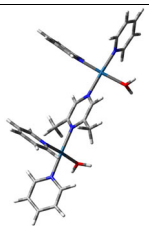
For all of the present complexes, the HOMOs are concentrated on the horizontal pyridyl π-acceptor carrier ligands and the LUMO is centred primarily on the pyrazine bridging ligand and partly on the d_{xy} orbital of the Pt centre. A general increase in the energy gap, ΔE (HOMO–LUMO) of the frontier orbitals, and a decrease in NBO charges, dependent on the position of the methyl group, are observed upon introducing an electron-donating methyl group to the pyrazine moiety. This is linked with the increase in electron density at the metal centre which results in destabilization of the molecular orbitals. Because of the outcome of twisting the pyridine rings to the equatorial plane as revealed in Table 1, the thermodynamic and kinetic data in this paper are discussed in line with the geometry-optimized structures.

Included in Table 2 are DFT-based reactivity descriptors such as chemical hardness, chemical potential and electrophilicity index which were calculated from the HOMO and LUMO energies [31–35] to elucidate the observed reactivity trend of the complexes. From Table 2, the chemical hardness decreases in the order **Pt-2,3PZN > Pt-2,5PZN > Pt-2,6PZN > Pt-PZN** and tallies well with the observed reactivity trend such that **Pt-PZN** is more reactive than **Pt-2,3PZN**. It is worth noting that the values of electronic chemical potential (Table 2), which describes the escaping tendency of electrons from an equilibrium system, are all of the same magnitude and negative. Generally, electrophilic (nucleophilic) species are characterized by high (low) magnitudes of the electronic chemical potential. In the present complexes, the magnitude of electronic chemical potential of **Pt-PZN** is slightly higher than that of **Pt-2,3PZN** by 0.33 eV, implying that **Pt-PZN** is more reactive than **Pt-2,3PZN**. The negative sign of the electronic potentials is expected because the electron acceptance by the complexes is accompanied by a decrease in energy. The electrophilicity trend that measures the capacity of a complex as a whole to accept electrons is **Pt-2,3PZN < Pt-2,5PZN < Pt-2,6PZN < Pt-PZN**. A good electrophile is characterized by a high value of electrophilicity index; therefore, **Pt-PZN** should be the most reactive complex in the series and **Pt-2,3PZN** the least reactive.

Acidity of the aqua complexes

Figure 2 shows an example of the spectral changes observed during the pH titration of **Pt-2,6PZN** with NaOH. The pK_a values of the coordinated aqua ligands were calculated from the pH profiles, an example of which is shown as an inset in Fig. 2. Fitting of the data to separate single sigmoidal functions (Boltzmann) using Origin 7.5®

Table 1 Geometry optimized structures and DFT-calculated (B3LYP/LACVP + **) HOMO and LUMO for the investigated complexes

Complex	HOMO	LUMO	Planarity
Pt-PZN			
Pt-2,3PZN			
Pt-2,5PZN			
Pt-2,6PZN			

software [23] gave pK_a values for the deprotonation of the protons of the coordinated aqua ligands. The values are summarized in Table 3, along with the pK_a values of analogous dinuclear Pt(II) complexes having *cis* NH_3 ligands at each metal centre for comparison. The overall titration process can be presented by the stepwise reactions given in Scheme 2.

The results in Table 3 clearly show a correlation between the pK_a values and electronic as well as steric demands of the pyrazine ligand linking the two Pt(II) centres. The pK_{a1} values of the deprotonation of the first coordinated aqua ligand increase in the order of $3.14 < 3.35 \approx 3.37 < 3.59$ for **Pt-PZN, Pt-2,3PZN, Pt-2,5PZN** and **Pt-2,6PZN**, respectively. The trend in pK_a values is associated with the electronic effects of methyl substituents on the pyrazine moiety, which through inductive effects results in the Pt–OH_2 bond being longer and increased pK_a values of the resultant complex. The second deprotonation step (Table 3) in all these complexes occurs at higher pH values than the first, which is attributed to the decrease in overall charge from +4 to +3 upon formation of the hydroxo species. Interestingly, the pK_a values for the first deprotonation step obtained in this study are slightly lower than those obtained for the analogous dinuclear complexes with an sp^3-hybridized ammine unit (NH_3) in the *trans* and *cis* positions relative to the leaving group [7, 14]. This may be attributed to the effect of the introduced pyridine rings, which helps to stabilize the electron density on the Pt(II) centre and the hydroxo ligand, as the pyridine is a poor σ-donor compared to NH_3 [36].

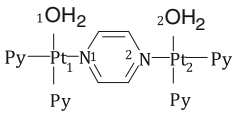
Kinetic measurements

As already mentioned, all the kinetic measurements were done under *pseudo* first-order conditions with respect to the nucleophile in order to force the reactions to completion. The substitution reactions of the complexes with thiourea nucleophiles (TU, DMTU, TMTU) were carried out at pH 2 and were characterized by two reaction steps (Scheme 3).Both substitution steps are irreversible, and the overall reaction can be summarized by the rate law given by Eq. 1.

Table 2 DFT-calculated parameters for the investigated Pt(II) complexes

	Pt-PZN	Pt-2,6PZN	Pt-2,5PZN	Pt-2,3PZN
HOMO–LUMO energy				
LUMO/eV	−14.10	−13.83	−13.64	−13.54
HOMO/eV	−17.26	−17.30	−17.16	−17.16
ΔE/eV	3.16	3.47	3.52	3.62
NBO Charges				
Pt_1	0.756	0.719	0.702	0.694
Pt_2	0.756	0.690	0.702	0.694
Chemical hardness (eV)	1.58	1.73	1.76	1.81
Chemical potential (eV)	−15.68	−15.56	−15.40	−15.35
Electrophilicity index (ω)	77.80	69.77	67.40	65.09
Bond Length (Å)				
Pt_1–Pt_2	7.033	7.045	7.039	7.027
Pt_1–N_1	2.105	2.128	2.114	2.119
Pt_2–N_2	2.105	2.105	2.116	2.119
Pt_1–OH_1	2.139	2.139	2.137	2.136
Pt_2–OH_2	2.139	2.134	2.136	2.136
Bond Angles (°)				
N_1–Pt_1–O_1	89.01	88.89	89.75	89.16
N_2–Pt_2–O_2	89.01	88.95	88.54	89.12
Point group symmetry	C_2	C_1	C_1	C_s

Numbering scheme is shown in Scheme 1



Scheme 1 Numbering Scheme followed for the present complexes

$$k_{obs1/2} = k_{1/2}[Nu] \quad (1)$$

The kinetic traces of the ligand substitution reaction for all complexes investigated gave excellent fits to a double exponential decay, yielding the *pseudo* first-order rate constants, k_{obs1} and k_{obs2} at specific nucleophile concentration and temperature for the first and second substitution step, respectively. An example of the kinetic trace obtained for the reaction of **Pt-2,3PZN** with TU is shown in Fig. 3.

The values of k_1 and k_2 were obtained from the slope of the plot of k_{obs1} or k_{obs2} against nucleophile concentration at 25 °C and are summarized in Table 4. Representative plots for the first and second substitution step for **Pt-PZN** with the three investigated nucleophiles are shown in Fig. 4 (also Figures SI 11, 13 and 15). The dependence of rate constant on temperature was studied between 15 and 35 °C. Typical Eyring plots are shown in Fig. 5 (also Figures SI 12, 14 and 16), and the activation parameters, $\Delta H^{\neq}$ and $\Delta S^{\neq}$, are presented in Table 4.

Discussion

Previous studies have shown that there is a relationship between pK_a values and electrophilicity of the metal centre [9, 11, 37–39]. It has also been reported that electron-withdrawing π-acceptor ligands tend to stabilize the electron-rich hydroxo species in comparison with the aqua species, resulting in lower pK_a values [11, 37, 38]. Alternatively, if the σ-donor capacity of the ligand *trans* to the aqua moiety is enhanced, then a higher pK_a value is obtained [40]. In this study, the pK_a results show that the introduction of methyl groups to the pyrazine moiety as in **Pt-2,3PZN**, **Pt-2,5PZN** and **Pt-2,6PZN** decreases the electrophilicity of the metal centre through electron donation via the pyrazine ring. This results in a moderate increase in pK_a values for these complexes compared to **Pt-PZN**. One can see that the position of the methyl groups in the pyrazine moiety of **Pt-2,3PZN** and **Pt-2,5PZN** gave equal distribution of the charges at each Pt(II) centre, explaining why these two complexes have very similar pK_a values. However, donation of charge from the methyl groups of **Pt-2,6PZN** is not symmetrical, resulting in Pt_1 being more electrophilic compared to Pt_2. This is in line with the large difference in pK_a values observed for this complex when compared with other complexes in this study. The trend in pK_a values is in good agreement with the DFT NBO calculated charges and the reactivity descriptors (Table 2).

Comparing the current pK_a findings with those of related *cis*-complexes [14] [*cis*-{$Pt(NH_3)_2(OH_2)$}$_2$-μ-pzn]$^{4+}$ (Table 3), the pK_a values obtained in this study were slightly lower. This indicates that the electron density on the PtOH moiety is less enhanced by the poor σ-donor pyridine rings [36] compared to NH_3 which is a strong σ-donor. Further observation also shows that deprotonation of the second aqua ligand occurs at higher pH values than the first step in all four complexes. This is ascribed to reduction of the overall charge from +4 to +3 following deprotonation of the first aqua ligand, causing a decrease in acidity and electrophilicity of the second Pt(II) centre. This increase in pK_a value due to the change in overall charge of the complex has also been observed in previous studies [1–14].

Substitution reactions of the series of dinuclear Pt(II) complexes with thiourea nucleophiles were monitored at pH 2 where all the complexes exist in their diaqua form and protonation of thiourea can be ruled out [41]. Two substitution steps were observed for all dinuclear Pt(II) complexes studied, indicating that there is electronic communication between the two Pt centres resulting in each having different kinetic properties. The smallness and rigidity of the azine linker enhances metal–metal electronic communication via electrostatic charge transfer

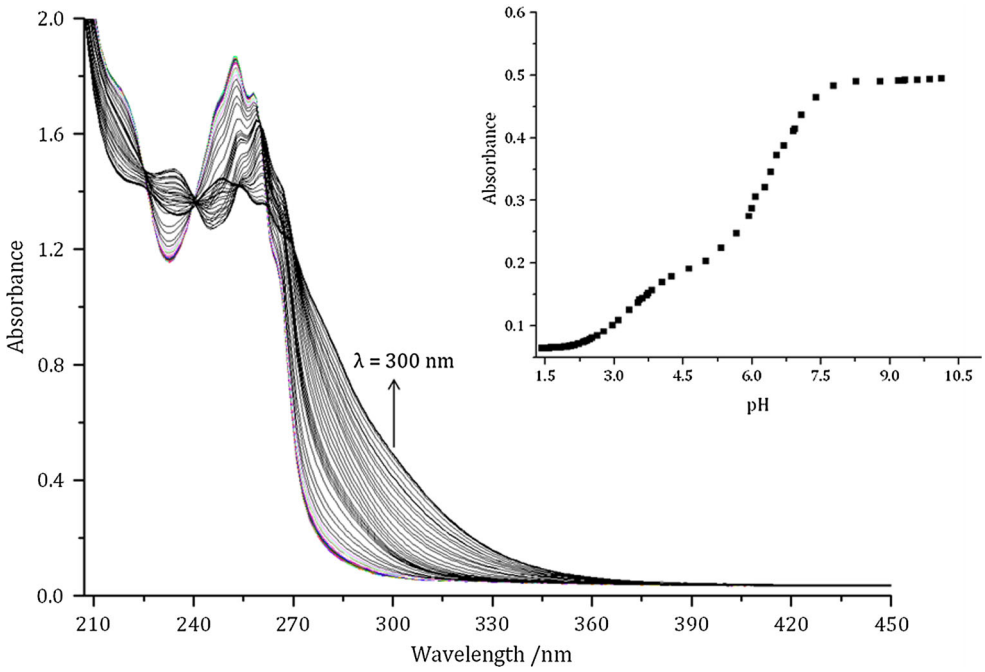
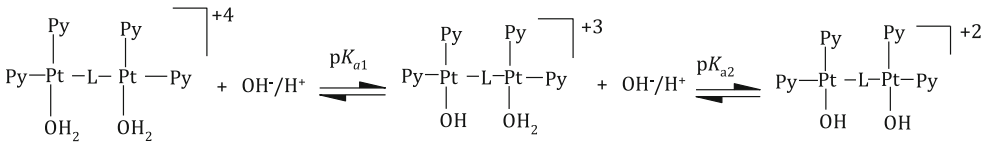


Fig. 2 UV–Vis spectra of the **Pt-2,6PZN** diaqua complex recorded as a function of pH in the range 1–10 at 25 °C. *Inset*: Plot of absorbance versus pH at 300 nm

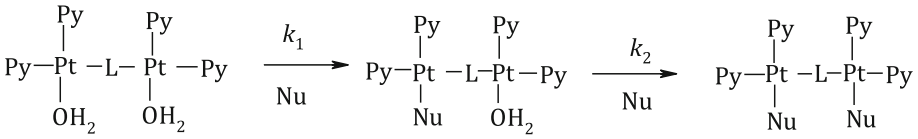
Table 3 The pK_a values for the deprotonation of Pt-bound aqua ligands in the dinuclear Pt(II) complexes

Complex	**Pt-PZN**	**Pt-2,6PZN**	**Pt-2,5PZN**	**Pt-2,3PZN**
pK_{a1}	3.14 ± 0.03	3.59 ± 0.03	3.37 ± 0.01	3.35 ± 0.01
	3.32 ± 0.06[a]	3.48 ± 0.51[a]	3.96 ± 0.12[a]	3.98 ± 0.11[a]
pK_{a2}	5.93 ± 0.04	6.12 ± 0.05	6.15 ± 0.02	6.43 ± 0.03
ΔpK_a	5.64 ± 0.09[a]	6.88 ± 0.04[a]	6.13 ± 0.05[a]	6.01 ± 0.18[a]
	2.79	2.84	2.78	2.77

[a] pK_a values extracted from Ref. [14]



Scheme 2 Stepwise deprotonation steps for the investigated complexes in an aqueous medium where Py = pyridine and L = bridge = pzn, 2,3-pzn, 2,5-pzn and 2,6-pzn



Scheme 3 The general reaction scheme for the reactions between the Pt(II) complexes and the thiourea nucleophiles at pH 2. Charges of the complexes are omitted for clarity and Py = pyridine and L = bridge = pzn, 2,3-pzn, 2,5-pzn and 2,6-pzn, Nu = nucleophile

from the metal to the lowest unoccupied molecular orbitals of the bridging ligand, making the Pt(II) centre more electrophilic [42]. It is worth mentioning that as previously reported [7, 14], the reactivity of such complexes is also dependent on the electronic and steric effect of the pyrazine linker.

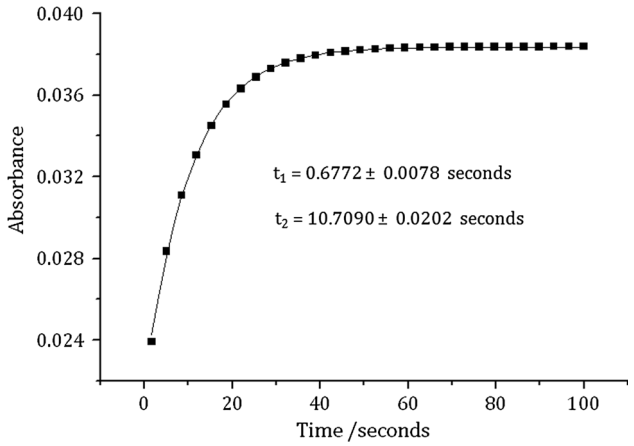


Fig. 3 Typical double exponential fit two step reaction between **Pt-2,3PZN** (0.2 mM) and TU (1.2 mM) recorded at 295 nm, $T = 298$ K, pH = 2.0, $I = 0.1$ M ($NaClO_4$) on the stopped-flow spectrophotometer

The first substitution step is assigned to the displacement of one aqua ligand with the thiourea nucleophile (TU, DMTU, TMTU), while the second step is assigned to substitution of the second aqua ligand. Since other dinuclear Pt(II) complexes studied in our group [14] were found to react via dechelation or dissociation of the linker, the ligand substitution of **Pt-2,5PZN-Cl$_2$** was followed using ^{1}H NMR to evaluate the possibility of dechelation. An array of the ^{1}H NMR spectra (showing only the aromatic resonances) for the reaction between **Pt-2,5PZN-Cl$_2$** and excess thiourea (6 equivalents) is shown in Fig. 6. The pyridyl protons were chosen to monitor the progress of the reaction as they are in close vicinity with the N-donor atom bonded to the metal centre and hence to the incoming TU. The numbering scheme employed for the pyridyl protons is shown in the structure of the **Pt-2,5PZN-Cl$_2$** complex in Scheme 4. From Fig. 6, the H_2 and $H_{2'}$ resonances of the

Table 4 Summary of rate constants and activation parameters of the investigated complexes for the first and second substitution steps

Complex	Nu	k_1/M^{-1} s^{-1}	k_2/M^{-1} s^{-1}	$\Delta H_1^{\neq}$/kJ mol^{-1}	$\Delta H_2^{\neq}$/kJ mol^{-1}	$\Delta S_1^{\neq}$/J K^{-1} mol^{-1}	$\Delta S_2^{\neq}$/J K^{-1} mol^{-1}
Pt-PZN	TU	427.7 ± 8.2	72.5 ± 1.1	27 ± 1	41 ± 1	−142 ± 4	−114 ± 3
	DMTU	393.3 ± 5.5	45.4 ± 1.0	41 ± 2	42 ± 2	−96 ± 6	−177 ± 7
	TMTU	102.4 ± 3.1	24.6 ± 0.5	49 ± 2	47 ± 1	−79 ± 6	−104 ± 3
Pt-2,6PZN	TU	338.7 ± 6.5	16.2 ± 0.3	40 ± 1	38 ± 2	−122 ± 3	−132 ± 6
	DMTU	200.6 ± 4.1	5.6 ± 0.1	43 ± 2	46 ± 2	−108 ± 6	−104 ± 6
	TMTU	146.1 ± 3.3	3.3 ± 0.05	48 ± 1	47 ± 2	−100 ± 4	−104 ± 5
Pt-2,5PZN	TU	314.0 ± 1.4	43.4 ± 0.6	27 ± 1	37 ± 2	−151 ± 3	−139 ± 6
	DMTU	304.7 ± 6.1	38.4 ± 0.6	26 ± 1	37 ± 2	−154 ± 3	−139 ± 6
	TMTU	102.2 ± 0.9	27.3 ± 0.3	39 ± 1	43 ± 2	−119 ± 3	−122 ± 6
Pt-2,3PZN	TU	247.8 ± 6.1	29.7 ± 0.7	31 ± 1	30 ± 1	−102 ± 3	−166 ± 3
	DMTU	185.5 ± 4.6	24.1 ± 0.7	30 ± 2	47 ± 3	−124 ± 6	−120 ± 9
	TMTU	136.1 ± 2.7	18.6 ± 0.6	43 ± 1	33 ± 2	−118 ± 3	−160 ± 6

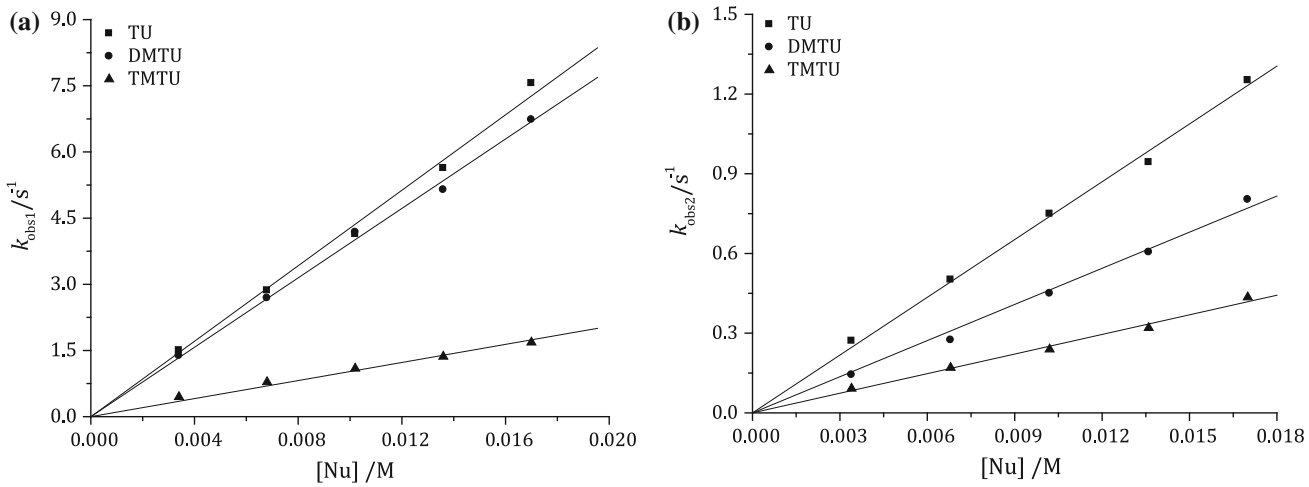


Fig. 4 Plots of $k_{obs1/2}$ versus nucleophile concentration for the **a** first and **b** second substitution steps of the reaction of 0.25 mM **Pt-PZN** at pH 2 and 25 °C ($I = 0.1$ M, $NaClO_4$)

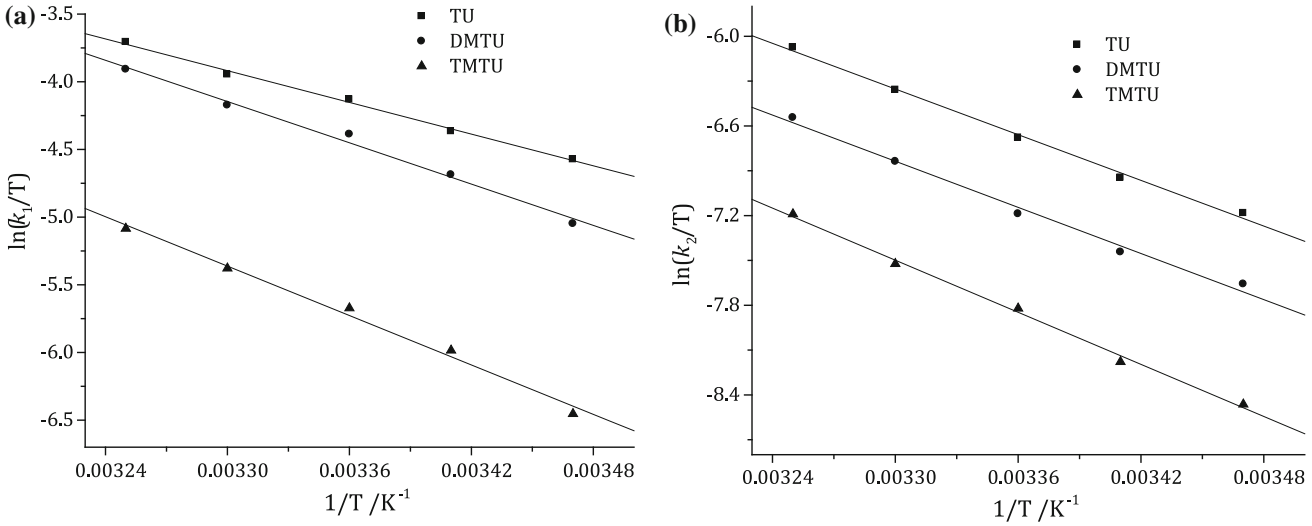


Fig. 5 Eyring plots for the determination of the thermal activation parameters for the **a** first and **b** second substitution steps of 0.25 mM **Pt-PZN** for all three nucleophiles studied at pH 2 ($I = 0.1$ M $NaClO_4$)

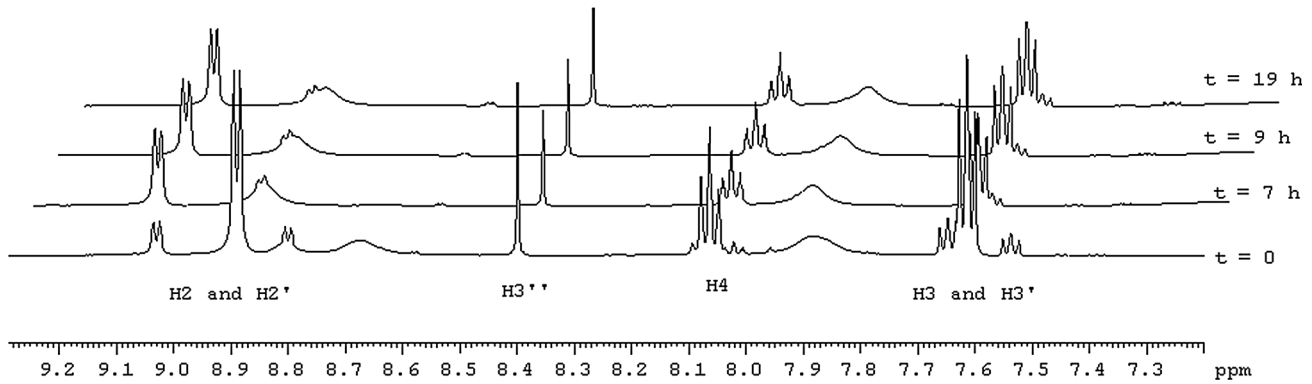
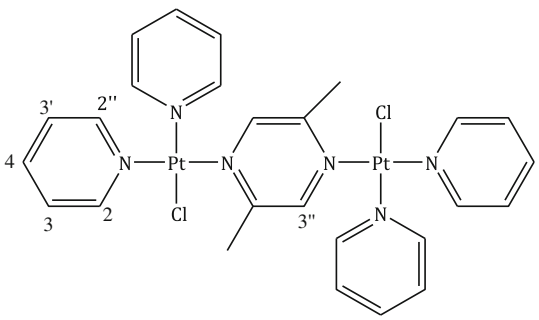


Fig. 6 ^{1}H NMR spectra of **Pt-2,5PZN-Cl$_2$** acquired during the reaction with 6 equivalents of TU at 30 °C. The first spectrum labelled $t = 0$ is for the unreacted **Pt-2,5PZN-Cl$_2$** and the rest are after the reaction with 6 equivalents of TU at the specified time



Scheme 4 The numbering scheme employed for the pyridyl protons of **Pt-2,5PZN-Cl$_2$**

pyridine in **Pt-2,5PZN-Cl$_2$** which appear at 8.89 ppm are shifted downfield to 9.07 ppm upon coordination of TU, while the electronic environments of the other pyridyl and pyrazine protons are not much affected by the coordination of thiourea. No other resonances in support of a dechelation process were observed during the progression of the reactions with TU for up to 19 h.

Taking the first substitution with thiourea as a reference, the reactivity of the dinuclear Pt(II) complexes decreases in the order $427.7 > 338.6 \simeq 314.0 > 247.8$ M^{-1} s^{-1} for **Pt-PZN, Pt-2,6PZN, Pt-2,5PZN** and **Pt-2,3PZN** respectively. This trend in reactivity can be explained in terms of the electronic and steric effects of the methyl groups introduced into the bridging ligand as reported in previous studies [7, 14]. The higher lability of the **Pt-PZN** complex is ascribed to both reduced steric hindrance and decreased electron density on the platinum centre caused by the π-acceptor ability of the pyrazine ligand and the twisted pyridine rings. This makes the metal centres in **Pt-PZN** more electrophilic and favour the rapid binding of the

entering nucleophile. The high reactivity of **Pt-PZN** is supported by the low pK_a values, narrow HOMO–LUMO gap, small value of chemical hardness and large values of electrophilicity index and NBO charges. The decrease in reactivity of the **Pt-2,6PZN**, **Pt-2,3PZN** and **Pt-2,5PZN** compared to **Pt-PZN** can be ascribed to the increased σ-inductive effects due to the additional methyl groups on the bridging pyrazine ligands consistent with previous studies [7, 13, 14, 43–45].

The second-order rate constant for **Pt-PZN** is greater than that for **Pt-2,6PZN** by a factor of ca. 1.3. These two complexes differ from each other in that one of the platinum centres in **Pt-2,6PZN** is hindered by methyl groups, making it less electrophilic compared to the second metal centre as supported by DFT-calculated NBO charges. From the NBO charges in Table 2, the electrophilicity of the unshielded metal centre of **Pt-2,6PZN** is of the same magnitude as that of **Pt-PZN**. This explains why the reactivity of the first substitution step in **Pt-2,6PZN** is close to that of **Pt-PZN** and higher than that of **Pt-2,5PZN** and **Pt-2,3PZN**. In addition, the determined pK_a values and the observed HOMO–LUMO gap for **Pt-2,6PZN** confirm the difference in electrophilicity between the two Pt(II) centres.

In the case of **Pt-2,3PZN** and **Pt-2,5PZN**, the positioning of the methyl groups in *ortho* and *para* positions on the pyrazine makes the two complexes symmetrical and the charges are equally distributed between the two Pt(II) centres. Hence, one expects the reactivity of these two complexes to be similar in magnitude. Surprisingly, this was not the case; it appears that the position of the methyl groups influences the twisting of the pyridine rings which in turn influences the extent of π-backbonding. The steric effect brought by the methyl groups in **Pt-2,3PZN** causes the twisting of the complex to the extent that the two Pt centres lie on a different plane by 9.1° (Figure **SI 20**) which interferes with the electronic communication and slows down the reactivity.

The second substitution step was significantly slower than the first in all the investigated complexes. This is possibly due to changes in the electronic communication between the two platinum atoms. The order of reactivity for the second substitution step with TU is **Pt-PZN** > **Pt-2,5PZN** > **Pt-2,3PZN** > **Pt-2,6PZN**. The same trend in reactivity is also observed for DMTU and TMTU. Similar to the first substitution step, this trend is explained by the increased σ-inductive effect of the methyl groups of the bridging pyrazine ligand which in turn increase its σ-donation to the metal centre and reduce its π-acceptability, resulting in a less-positive metal centre. The incoming nucleophile is then repelled by the increased electron density at the metal centre, leading to a less stable five-coordinate transition state. In the case of **Pt-2,6PZN**, there is an additional steric effect which blocks entry of the incoming nucleophile on both sides of the hindered Pt(II) centre, as supported by the reduced NBO charges of the second metal centre.

Comparing the reactivity of the **Pt-pzn** derivatives for both substitution steps with [*cis*-{$Pt(NH_3)_2(OH_2)$}$_2$-μ-pzn]$^{4+}$ and [*trans*-{$Pt(NH_3)_2(OH_2)$}$_2$-μ-pzn]$^{4+}$, its second-order rate constants are higher by factor of 10 and 23, respectively [7, 14]. This indicates that the structure containing pyridyl units labilizes the aqua ligands more than their *cis* and *trans*-counterparts with NH_3 as the ligand. The introduction of pyridine groups into [*cis*-{$Pt(NH_3)_2(OH_2)$}$_2$-μ-pzn]$^{4+}$ changes the geometry of the complex in such a way that a significant increase in π-acceptor abilities of the ligands is induced. The net outcome is a significant increase in the electrophilicity of the complex, as reflected by a more positive charge on the Pt(II) centres, high electrophilicity indices and lower pK_a values for the deprotonation of the aqua ligands. This increases the rate of substitution of the coordinated aqua ligands. In addition, from Table 1, the HOMO in all these dinuclear complexes is located on the pyridine ligand and the LUMO is largely centred on the pyrazine bridging ligand. The HOMO of the previously studied pyrazine bridged dinuclear Pt(II) complexes [7, 14] was located on the metal centres as the NH_3 is a better σ-donor than pyridine, making the Pt(II) centres less electrophilic compared to the current Pt(II) complexes.

The dependence on the rate of substitution of the aqua ligand on the steric hindrance of the incoming nucleophiles is clearly evident from the results shown in Table 4. Substitutions involving TMTU gave the lowest rates, whereas those with TU reacted significantly faster. This trend is in line with the size of TMTU nucleophile relative to TU and DMTU [39, 46, 47]. The activation parameters in Table 4 show that the entropies of activation are large and negative. This indicates that the transition state is highly ordered and more compact than either the reactant or product species. In addition, the enthalpies of activation are relatively low, showing the ease with which the new bond can form due to the electrophilicity of the metal centre. These activation parameters are consistent with substitution reactions for square-planar Pt(II) complexes which are known to proceed via an associative mechanism [48].

Conclusions

Novel dinuclear Pt(II) complexes were synthesized, and their kinetic substitution reactions undertaken. It was found that the use of pyridine ligands instead of NH_3 in $Pt(NH_3)_2(OH_2)$}$_2$-μ-pzn]$^{4+}$ increases the substitution rates of the diaqua complexes by a factor of 10 and 23 for the *cis* and *trans* complexes, respectively, while retaining an associative mode of substitution. This is because pyridine

enhances the π-backbonding by accepting the electrons from the metal centres to the empty π*-orbitals of the pyridine subunits. This is made possible due to the geometry of these complexes that results in the pyridine, pyrazine and Pt centre all being on the same plane. This results in lower pK_a values, increased electrophilicity of the Pt(II) centre and an increase in reactivity of the metal, as supported by DFT calculations. The trends in these azine-bridged Pt(II) complexes are the same as those reported for [{*cis/trans*-$Pt(NH_3)_2(OH_2)$}$_2$(μ-pzn)]$(ClO4)_4$ complexes containing NH_3 ligands [7, 14]. Electron-donating groups such as methyl as used in this study not only supply electrons in the pyrazine bridge but also impart steric hindrance against incoming nucleophiles.

Electronic Supplementary Information

The available ESI includes a number of NMR and mass spectra, wavelengths for kinetic measurements, pH titration spectra, concentration dependence and Eyring plots for determination of second-order rate constants and activation parameters, respectively, HOMO–LUMO energy diagrams and planarity of the investigated complexes.

Acknowledgments The authors thank the University of Dar es Salaam (Tanzania) and University of KwaZulu-Natal (South Africa) for financial support to Grace Kinunda.

References

1. Mambanda A, Jaganyi D, Hochreuther S, van Eldik R (2010) Dalton Trans 39:3595
2. Mambanda A, Jaganyi D (2012) Dalton Trans 41:908
3. Hochreuther S, van Eldik R (2012) Inorg Chem 51:3025
4. Hochreuther S, Puchta R, van Eldik R (2011) Inorg Chem 50:8984
5. Soldatović T, Jovanović S, Bugarčić ŽD, van Eldik R (2012) Dalton Trans 41:876
6. Hochreuther S, Puchta R, van Eldik R (2011) Inorg Chem 50:12747
7. Reddy D, Jaganyi D (2011) Int J Chem Kinet 43:161
8. Jaganyi D, Munisamy VM, Reddy D (2006) Int J Chem Kinet 38(3):202
9. Ertürk H, Hofmann A, Puchta R, van Eldik R (2007) Dalton Trans 2295
10. Ertürk H, Maigut J, Puchta R, van Eldik R (2008) Dalton Trans 2759
11. Hofmann A, van Eldik R (2003) Dalton Trans 2979
12. Ertürk H, Puchta R, van Eldik R (2009) Eur J Inorg Chem 1334
13. Ongoma P, Jaganyi D (2014) Trans Met Chem 39:407
14. Jaganyi D, Ongoma P (2013) Dalton Trans 42:2724
15. Zou Y, Van Houten B, Farrell N (1993) Biochemistry 32:9632
16. Farrell N, Appleton TG, Qu Y, Roberts JD, Soares Fontes AP, Skov KA, Wu P, Zou Y (1995) Biochemistry 34:15480
17. Kasparková J, Novaková O, Marini V, Najajreh Y, Gibson D, Perez J-M, Brabec V (2003) J Biol Chem 278(48):47516
18. Kalinowska-Lis U, Ochocki J, Matlawska-Wasowska K (2008) Coord Chem Rev 252:1328
19. Farrer NJ, Woods JA, Salassa L, Zhao Y, Robinson KS, Clarkson G, Mackay FS, Sadler PJ (2010) Angew Chem Int Ed 49:8905
20. Hollis LS, Amundsen AR, Stern EW (1989) J Med Chem 32:128
21. Qu Y, Farrell N (1992) Inorg Chem 31:930
22. Jansen BAJ, van der Zwan J, den Dulk H, Brouwer J, Reedijk J (2001) J Med Chem 44:245
23. Origin$^{7.5TM}$ SRO, v7.5714 (B5714), Origin Lab Corporation, Northampton, One, Northampton, MA, 01060, USA, 2003
24. Becke AD (1993) J Chem Phys 98:5648
25. Wadt WR, Hay PJ (1985) J Chem Phys 82:284
26. Frisch MJ, Trucks GW, Schlegel HB, Scuseria GE, Robb MA, Cheeseman JR, Scalmani G, Barone V, Mennucci B, Petersson GA, Nakatsuji H, Caricato M, Li X, Hratchian HP, Izmaylov AF, Bloino J, Zheng G, Sonnenberg JL, Hada M, Ehara M, Toyota K, Fukuda R, Hasegawa J, Ishida M, Nakajima T, Honda Y, Kitao O, Nakai H, Vreven T, Montgomery JA, Peralta JE, Ogliaro F, Bearpark M, Heyd JJ, Brothers E, Kudin KN, Staroverov VN, Kobayashi R, Normand J, Raghavachari K, Rendell A, Burant JC, Iyengar SS, Tomasi J, Cossi M, Rega N, Millam JM, Klene M, Knox JE, Cross JB, Bakken V, Adamo C, Jaramillo J, Gomperts R, Stratmann RE, Yazyev O, Austin AJ, Cammi R, Pomelli C, Ochterski JW, Martin RL, Morokuma K, Zakrzewski VG, Voth GA, Salvador P, Dannenberg JJ, Dapprich S, Daniels AD, Farkas O, Foresman JB, Ortiz JV, Cioslowski J, Fox DJ (2009) Gaussian 09, Revision A.1. Gaussian, Inc., Wallingford
27. Barone V, Cossi M (1995) J Phys Chem A 102
28. Cossi M, Scalmani G, Rega N, Barone V (2003) J Comput Chem 24:669
29. Lee G-Y, Jun M-S (2001) Bull Korean Chem Soc 22(1):11
30. Eyring H (1935) J Chem Phys 3:107
31. Mebi CA (2011) J Chem Sci 123(5):727
32. Jaramillo P, Domingo LR, Pérez P (2006) www.captura.uchile.cl/jspui/bitstream/2250/5781/1/Jaramillo_P.pdf
33. Cedillo A, Contreras R (2012) J Mex Chem Soc 56(3):257
34. Parr RG, Szentpály LV, Liu S (1922) J Am Chem Soc 1999:121
35. Parthasarathi R, Subramanian V, Roy DR, Chattaraj PK (2004) Bioorg Med Chem 12:5533
36. Katritzky AR, Pozharski AF (2000) Handbook of heterocyclic chemistry, 2nd edn. Elsevier, Pergamon, pp 177–178
37. Hofmann A, Jaganyi D, Munro OQ, Leihr G, van Eldik R (2003) Inorg Chem 42:1688
38. Jaganyi D, Hofmann A, van Eldik R (2001) Angew Chem Int Ed 40:1680
39. Jaganyi D, Reddy D, Gertenbach J-A, Hofmann A, van Eldik R (2004) Dalton Trans 299
40. Schmülling M, Grove DM, van Koten G, van Eldik R, Veldman N, Spek AL (1996) Organometallics 15:1384
41. Schiessl WC, Summa NK, Weber CF, Gubo S, Dücker-Benfer C, Puchta R, Eikem Hommes NJR, van Eldik R (2005) Z Anorg Allg Chem 631:2812
42. Field JS, Gertenbach J-A, Haines RJ, Munro OQ, McMillin DR (2007) Z Naturforsch 62:447
43. Jaganyi D, Pantoja E, Gallipoli A, van Zutphen S, Komeda S, Reddy D, Lutz M, Tooke DM, Spek AL, Navarro-Ranninger C, Reedijk J (1955) J Inorg Biochem 2006:100
44. Hofmann A, Dahlernburg L, van Eldik R (2003) Inorg Chem 42:6528
45. Pasini A, Rigamonti L, Forni A, Manassero M, Manassero C (2010) Inorg Chem 49:123
46. Jaganyi D, Tiba F (2003) Transition Met Chem 28:803
47. Reddy D, Jaganyi D (2006) Transition Met Chem 31:792
48. Tobe ML, Burgess J (1999) Inorganic reaction mechanisms, Addison Wiley, Longman, Ltd., Essex, pp 30–33, 70–112